



# Controls on ecosystem water-use and water-use efficiency: Insights from a comparison between grassland and riparian forest in the northern Great Plains



Hao Yang<sup>a,b</sup>, Stewart B. Rood<sup>a</sup>, Lawrence B. Flanagan<sup>a,\*</sup>

<sup>a</sup> Department of Biological Sciences, University of Lethbridge, Water & Environmental Science Building, 4401 University Drive, Lethbridge, Alberta, T1K 3M4, Canada

<sup>b</sup> Key Laboratory of Ecosystem Network Observation and Modeling, Institute of Geographic Sciences and Natural Resources Research, Chinese Academy of Sciences, Beijing, 100101, China

## ARTICLE INFO

### Keywords:

Eddy covariance  
*Populus* spp.  
 Gross ecosystem photosynthesis  
 Stomatal conductance  
 Leaf area index  
 Soil moisture

## ABSTRACT

Within the grassland-dominated landscape of the North American Great Plains, riparian forest ecosystems exist along river floodplains. We compared cumulative evapotranspiration (ET) and ecosystem water-use efficiency (WUE) between a cottonwood forest and a nearby native grassland ecosystem in southern Alberta, using eddy covariance measurements during May–September (growing season) of three study years. Our objective was to test predictions about mechanistic controls on ecosystem water-use, and to provide insights into the amount of alluvial groundwater and stored soil water required to support a healthy riparian forest within the Great Plains biome. Grassland ET was dependent on precipitation inputs during the growing season. Cumulative growing season ET at the cottonwood site (375–451 mm) exceeded grassland ET (111–213 mm) by 2.1- to 3.4-fold depending on study year, despite slightly higher WUE in the cottonwood ecosystem. The difference in cumulative ET between ecosystems ranged from 238 to 264 mm in different years, in a region that normally receives 258 mm of cumulative precipitation during May–September. The large ET at the cottonwood site was caused by two-fold higher LAI, and associated greater canopy conductance than was apparent at the grassland site. The additional soil water required for the higher cottonwood ET was supplied by access to alluvial groundwater, which is recharged by river water, and was also supported by a larger soil volume to store water from precipitation and river flooding inputs. These factors resulted in a relatively long interval for cottonwood photosynthetic gas exchange that was consistent among years despite widely different environmental conditions, while the grassland had shorter growing season lengths that were constrained further as precipitation and soil moisture declined among years. Our analyses contribute to understanding the water requirements of these contrasting ecosystems and will help to improve management procedures for regulating river flow rates in order to sustain healthy riparian cottonwood ecosystems.

## 1. Introduction

The Great Plains is the second largest biome in North America and extends south from the aspen parkland and boreal forest areas in Alberta and Saskatchewan, Canada through the USA to New Mexico and Texas (Ostlie et al., 1997; Zhang et al., 2011). There is a substantial west to east gradient in precipitation that divides the native vegetation of the Great Plains into short-, mid- and tall grasslands or prairie ecosystems (Heisler-White et al., 2009; Wilcox et al., 2015). Productivity and water-use in prairie grassland ecosystems are strongly controlled by the amount of summer precipitation inputs, although the size of rain events and the interval between rain events can also significantly

influence grassland ecosystem physiology (Knapp and Smith, 2001; Heisler-White et al., 2008, 2009; Knapp et al., 2008). Within this grassland-dominated landscape, riparian ecosystems also exist along the floodplains of rivers that distribute snow-melt water from the Rocky Mountains as they flow out through the prairies (Rood et al., 2003). Within the northern Great Plains of southern Alberta, river water also flows laterally out of the main river channels (“losing rivers”) creating an alluvial aquifer below the river floodplain (Hauer et al., 2016). A variety of important ecological processes connect the aquatic and terrestrial ecosystems through this alluvial aquifer and these ecological interactions promote regional biodiversity across the full spectrum from microbes to vertebrate animals (Hauer et al., 2016). Riparian

\* Corresponding author.

E-mail address: [larry.flanagan@uleth.ca](mailto:larry.flanagan@uleth.ca) (L.B. Flanagan).

<https://doi.org/10.1016/j.agrformet.2019.02.034>

Received 26 April 2018; Received in revised form 14 November 2018; Accepted 24 February 2019

0168-1923/ © 2019 Elsevier B.V. All rights reserved.

cottonwood forests develop on these floodplains within the semiarid landscape that is otherwise treeless, in part supported by the alluvial groundwater which supplements any precipitation inputs to the soil (Snyder and Williams, 2000; Rood et al., 2003; Scott et al., 2003, 2000; Flanagan et al., 2017). The riparian forest ecosystems contribute many valued ecosystem services (Naiman et al., 2005; Hauer et al., 2016), but their health and survival has been threatened by reductions in river flows associated with dams that divert river water for agricultural irrigation, municipal and industrial consumption (Rood et al., 1995, 2003, 2005, 2008; Schindler and Donahue, 2006). This raises the fundamental question, how much river water is required to support healthy riparian forest ecosystems within the Great Plains biome? In order to help answer this question, and to provide some ecological perspective on the water-use requirements of riparian cottonwood forest ecosystems, our major objective in this study was to compare water-use and water-use efficiency between a native grassland ecosystem and a native, riparian cottonwood ecosystem in the northern Great Plains of southern Alberta. This comparison should provide insights into the amount of river water required to support a healthy riparian forest ecosystem in this region, as the local grasslands were expected to rely only on water sourced from summer precipitation inputs (Wever et al., 2002). More generally, this analysis would allow evaluation of some important factors influencing water-use and water-use efficiency in these two ecosystems.

In this paper we define water-use as cumulative ecosystem evapotranspiration (ET) during the growing season, and water-use efficiency (WUE) as the ratio of ecosystem photosynthesis to ecosystem ET. Several ecological and physiological factors can control ecosystem water-use and WUE, including: leaf area index (LAI), stomatal conductance, precipitation input, soil moisture content, access to groundwater, temperature, vapor pressure difference (VPD), and growing season length (Kelliher et al., 1995; Ponton et al., 2006; Beer et al., 2009). We predicted that cottonwood riparian forests and native grassland ecosystems should differ for several of these factors, as is described below. The contrasting dominant plant functional types associated with cottonwood forests and native prairie grassland will result in important differences in leaf and canopy photosynthetic gas exchange processes. Broad-leaf deciduous trees tend to have lower ratios of stomatal conductance to photosynthetic capacity than  $C_3$  grasses (Smedley et al., 1991; Brooks et al., 1997), but the typically larger LAI of forests than grasslands results in canopy conductance being higher in the forest ecosystems (Kelliher et al., 1995; Wever et al., 2002; Flanagan et al., 2017). While precipitation input will be the same in nearby riparian forest and grassland ecosystems, groundwater access by deep-rooted, phreatophytic cottonwood trees should increase the supply of water to riparian forests above that available to grasslands (Scott et al., 2003, 2004). In addition, the depth of soil and permeable substrate beneath floodplain forests (2–3 m) exceeds that of native grasslands in the northern Great Plains (0–30 cm), and so the riparian forests should have greater soil water storage capacity. Local forest and grassland ecosystems are exposed to similar aerial environmental conditions (photosynthetically active radiation, temperature, VPD), but they differ in ecological strategies of the dominant plant functional types. In addition, the differing amounts of available soil water can result in contrasting growing season lengths for forest and grassland ecosystems. Grassland plants grow fast and use water quickly when it is readily available and then go dormant to survive times of water shortages (Flanagan and Adkinson, 2011). This ecological strategy of grassland plants can result in significantly shorter active growing seasons than is apparent for riparian forest ecosystems.

In this study, we compared ecosystem water-use and WUE between nearby riparian cottonwood forest and native grassland ecosystems in southern Alberta using eddy covariance measurements. Our goal was to test these predictions made above about mechanistic controls on ecosystem water-use, and to provide insights into the amount of alluvial groundwater and stored soil water that is required to support a healthy

riparian forest ecosystem within the Great Plains biome. The study was conducted during May–September in three different years that had contrasting precipitation, air temperature and VPD, and so provided perspective on summertime environmental controls that influence water-use and WUE in riparian forest and grassland ecosystems in the northern Great Plains biome.

## 2. Materials and methods

### 2.1. Study site descriptions

The two study sites were located in Lethbridge, Alberta, Canada near the northwestern limit of the Great Plains biome. The mean annual temperature for Lethbridge was 5.7 °C and average annual precipitation was 386.3 mm (1971–2010: Canadian Climate Normals, Environment Canada; climate.weather.gc.ca/climate\_normals/). The forest site was a riparian cottonwood forest in the Helen Schuler Nature Reserve (HSNR, 49.702 °N, 112.863 °W, elevation 928 m) within the Oldman River valley (Flanagan et al., 2017). This forest was dominated by plains cottonwood (*Populus deltoides* W. Bartrum ex Marshall), narrow-leaf cottonwood (*Populus angustifolia* James), balsam poplar (*P. balsamifera* L.), black cottonwood (*P. trichocarpa* Torr. & A. Gray) and their natural, interspecific hybrids (Gom and Rood, 1999; Rood et al., 2013). Average tree height was  $18 \pm 5$  m (mean  $\pm$  SD,  $n = 60$ ), tree diameter at breast height (1.35 m) was  $37 \pm 15$  cm, average tree density was  $276 \pm 300$  trees per hectare (mean  $\pm$  SD), and peak LAI in 2014 was  $1.8 \text{ m}^2 \text{ m}^{-2}$  (Flanagan et al., 2017). The grassland site (49.471 °N, 112.940 °W, elevation 951 m) was 5.7 km distant from the cottonwood forest site, had flat terrain, and the soil was underlain by a thick glacial till with very low permeability and no water table (Flanagan and Adkinson, 2011). The dominant species were northern wheatgrass (*Agropyron dasystachyum* (Hook) Scribn. & J.G. Sm.) and western wheatgrass (*Agropyron smithii* (Rydb.) Á. Löve), and peak LAI in 2014 was  $1.0 \text{ m}^2 \text{ m}^{-2}$  (Flanagan et al., 2002; Flanagan and Johnson, 2005; Flanagan and Adkinson, 2011). The site included native prairie that had never been cultivated and had minimal livestock grazing, with no grazing for at least 35 years.

### 2.2. Meteorological and eddy covariance flux measurements

The instruments and procedures for meteorological and eddy covariance (EC) flux measurements for  $\text{CO}_2$ , water vapor (latent heat) and sensible heat have been previously described in detail for both the cottonwood forest (Flanagan et al., 2017) and grassland site (Flanagan and Adkinson, 2011). For background we also include some basic information on the eddy covariance equipment in the following text. At the cottonwood forest, the sonic anemometer (CSAT3, Campbell Scientific, Edmonton, AB, Canada) was mounted on an instrumentation tower at 22 m above ground. An infrared gas analyzer (LI-7200, LI-COR Inc., Lincoln, NE, USA) measured changes in  $\text{CO}_2$  and  $\text{H}_2\text{O}$  molar densities in an air flow of  $14 \text{ L min}^{-1}$  that was pulled by the flow module (LI-7200-101, LI-COR Inc.) through 1 m of Decabon tubing to the analyzer, with the tubing inlet attached to the bottom support arm of the sonic anemometer. The signals from the sonic anemometer and gas analyzer were sampled at 10 Hz by an analyzer interface unit (LI-7550, LI-COR Inc.) and stored on a memory drive. At the grassland site, the sonic anemometer (R3, Gill Instruments Ltd., Lymington, UK) was mounted on a support scaffold at a height of 6 m above ground. The infrared gas analyzer (LI-7000, LI-COR Inc.) was located in a temperature-controlled housing and used to measure changes in  $\text{CO}_2$  and  $\text{H}_2\text{O}$  mixing ratios after air was drawn through 3 m of tubing to the analyzer ( $17 \text{ L min}^{-1}$ ) by a diaphragm pump (UN828 KNI, KNF Neuberger Inc., Trenton, NJ, USA) placed downstream of the analyzer. The signals from the sonic anemometer and gas analyzer were recorded at 20 Hz on a computer located in a temperature-controlled hut at the site. The EC system was operational at the cottonwood site during the

growing season months of 2014 (May–October), 2015 (May–August) and 2017 (May–September), although flux data were not collected during the period of over-bank flooding of Oldman River in June 17–July 1, 2014 and due to LI-7200 instrument malfunction during July 28–August 22, 2014. The grassland EC system was functional during almost all 30-minute time periods from 2014 through 2017. The fetch at the grassland site was a minimum of 300 m to the east (wind from this direction only occurred infrequently) and extended from 500 to 1000 m in all other directions. At the cottonwood forest, the fetch was 400 m in both north and south directions and 300 m directly west of the tower. Fetch was only 80 m east of the tower, but data collected when the wind originated from the sector between 45–135° (infrequent wind direction) was removed before any analyses were conducted. Flux footprint calculations at the cottonwood site indicated that the average horizontal distance to the peak contribution for the measured eddy covariance fluxes was at  $120 \pm 5$  m, while the distance within which 90% of the fluxes originated was  $330 \pm 26$  m. So the vast majority of the measured eddy fluxes originated within the cottonwood forest, except when the wind came from the excluded wind sector (Flanagan et al., 2017).

### 2.3. Growing season ecosystem water budget calculations

The process of gap-filling missing ET data for water budget calculations was done using the Penman–Monteith equation (Monteith, 1965). In order to calculate canopy conductance for use in the Penman–Monteith equation, we developed linked leaf phenology and stomatal conductance models (Flanagan et al., 2017). The development of the leaf phenology model was guided by two empirical observations. First, there are strong physiological links among leaf photosynthetic capacity, stomatal conductance and hydraulic conductance (Wong et al., 1979; Katul et al., 2003). Second, canopy gross photosynthesis rates in broad-leaf deciduous trees and grass tend to decline as leaves age after the seasonal peak, even while canopy LAI measurements remain at peak values (Keenan et al., 2014). Therefore we used gap-filled, daily-integrated calculations of gross ecosystem photosynthesis ( $g C m^{-2} day^{-1}$ ) as a proxy for describing temporal variation in functional leaf area. The procedures used for partitioning eddy covariance measurements (30-minute average values) of net ecosystem  $CO_2$  exchange into total ecosystem respiration and gross ecosystem photosynthesis (GEP) and gap-filling the GEP values have been described previously (Flanagan et al., 2017 for the cottonwood site; Flanagan and Adkinson, 2011 for the grassland site). Full details of the functional leaf phenology model are outlined in Flanagan et al. (2017). The same phenology model and its parameters were used for both the grassland and cottonwood sites.

To develop a model for stomatal conductance we first produced a set of surface or canopy conductance calculations that were obtained by inverting the Penman–Monteith equation (Monteith, 1965) as described earlier (Wever et al., 2002; Flanagan et al., 2017). At the grassland, previous calculations of the decoupling coefficient (Jarvis and McNaughton, 1986) indicated strong control of evapotranspiration by canopy conductance (Wever et al., 2002). Decoupling coefficient values are typically lower in forest than grassland ecosystems because of the associated higher magnitude of aerodynamic roughness and boundary layer conductance in forest ecosystems (Jarvis and McNaughton, 1986). So we assume that in both of our study ecosystems, evapotranspiration was strongly controlled by canopy conductance. Our canopy conductance calculations made use of the following inputs: (i) evapotranspiration rates measured by eddy covariance and (ii) the associated environmental conditions, that had been bin-averaged by time of day for separate monthly data (May–July) collected in 2014, 2015, and 2017. Thus, we generated nine sets of the mean diurnal pattern of canopy conductance for both the forest and grassland sites, one for each month in all three study years. The associated mean diurnal pattern of stomatal conductance was determined by dividing the monthly canopy conductance values by the average absolute functional leaf area index

values for each month (May–June) calculated with the functional leaf phenology model (i.e. canopy conductance ( $mmol m^{-2} s^{-1}$ ; ground area) = stomatal conductance ( $mmol m^{-2} s^{-1}$ ; leaf area)  $\times$  LAI ( $m^2 m^{-2}$ ; leaf area per ground area). For each site, the combined nine sets of data for the mean diurnal pattern of stomatal conductance were used to develop and parameterize a stomatal conductance model as described below.

We used the Jarvis (1976) model for stomatal conductance ( $g$ ,  $mmol m^{-2} s^{-1}$ ):

$$g = g_{max} f(Q) f(A_w) \quad (1)$$

where  $g_{max}$  is a maximum value of stomatal conductance ( $mmol m^{-2} s^{-1}$ ),  $f(Q)$  and  $f(A_w)$  are functions that vary between 0 and 1 and describe the response of stomatal conductance to incident photosynthetic photon flux density ( $Q$ ,  $\mu mol m^{-2} s^{-1}$ ) and available soil moisture ( $A_w$ , unit less), respectively. The  $g_{max}$  value was calculated as a function of vapor pressure deficit ( $D$ , hPa) using the equation proposed by Lloyd (1991):

$$g_{max} = \frac{1}{k_D (D)^{0.5}} \quad (2)$$

where  $k_D$  is a fitted constant. The  $f(Q)$  function was based on an equation used to describe electron transport (Harley et al., 1992):

$$f(Q) = \left( \frac{Q\alpha}{1 + \frac{Q^2\alpha^2}{g_{max}^2}} \right) \left( \frac{1}{g_{max}} \right) \quad (3)$$

where  $\alpha$  is a fitted constant. Eq. (4) was used for the response of stomatal conductance to available soil moisture,  $f(A_w)$ :

$$f(A_w) = \left( \frac{(A_w - 0)(A_w - Max)}{(A_w - 0)(A_w - Max) - (A_w - Opt)^2} \right) \quad (4)$$

where  $A_w$  is available soil moisture, a relative measure calculated based on the soil volumetric moisture measurements (made using calibrated readings from soil water reflectometers (CS616, Campbell Scientific) at both study sites). At the cottonwood site, soil water content measurements were made at four depths through the soil profile and integrated vertically to calculate the total moisture content in the upper 2.5 m of soil (Flanagan et al., 2017). The maximum integrated soil water content (1577 mm) was recorded at the cottonwood site during the flood conditions of June 2014, and the minimum (250 mm) value was estimated from the permanent wilting point in the soil type at the site. For the grassland site, the maximum ( $0.45 m^3 m^{-3}$ ) and minimum ( $0.10 m^3 m^{-3}$ ) volumetric soil water contents were those recorded for the soil depth interval 0–15 cm during a decade of sampling at the site (1998–2008; Flanagan and Johnson, 2005; Flanagan and Adkinson, 2011). Available soil moisture ( $A_w$ ) was specifically defined as the ratio of actual available soil water (difference between a given daily measurement and the minimum soil water content) to maximum available soil water (difference between maximum and minimum soil water contents).  $Opt$  is a fitted constant, the value of  $A_w$  at which  $f(A_w)$  is at its maximum (1), and  $Max$  is a fitted constant, the maximum value of  $A_w$  that results in the return of the  $f(A_w)$  function to zero, and acts to define the shape of the  $f(A_w)$  function.

Non-linear least-squares regression was used to obtain estimates of the parameters  $k_D$ ,  $\alpha$ ,  $Opt$  and  $Max$  with Matlab software (R2014a, The Mathworks Inc., Natick, MA, USA). The stomatal conductance model was fit to the nine monthly sets of the mean diurnal pattern of stomatal conductance and associated environmental data for each site. The following values were calculated for the stomatal conductance model constants: for the cottonwood site,  $k_D = 8.61 \times 10^{-4}$ ,  $\alpha = 0.431$ ,  $Opt = 0.769$ ,  $Max = 1.066$ ; for the grassland site,  $k_D = 17.10 \times 10^{-4}$ ,  $\alpha = 0.800$ ,  $Opt = 0.959$ ,  $Max = 1.000$ .

As noted above, gap-filling of missing EC data for water budget calculations was done using the Penman–Monteith equation to calculate ecosystem ET. These gap-filling ET calculations were done using gap-

**Table 1**

Comparison of daily average ( $\pm$  SD) air temperature and vapor pressure deficit (VPD) in Lethbridge, Alberta during 2014, 2015, 2017. The daily average calculations only made use of the half-hour time periods between 10:00 and 17:00 h in June and July (days 152–212,  $n = 61$ ). Significant differences were apparent among years for both air temperature and VPD based on one-way ANOVA, (air temperature:  $F(2, 180) = 8.64, P < 0.001$ ; VPD  $F(2, 180) = 23.15, P < 0.001$ ).

	2014	2015	2017
Air Temperature ( $^{\circ}\text{C}$ )	$21.0 \pm 4.9$	$23.3 \pm 4.9$	$24.7 \pm 5.0$
VPD (kPa)	$1.5 \pm 0.7$	$2.2 \pm 0.9$	$2.5 \pm 1.0$

filled meteorological data from both study sites, and calculations of seasonal variation in canopy conductance determined using the functional leaf phenology and stomatal conductance models described above. We observed strong correlation between measurements of ecosystem ET and calculations of ET using the Penman-Monteith equation, examples of which are shown in Figs. 3 and 4.

#### 2.4. Daily and seasonal ecosystem water-use efficiency

We calculated seasonally-integrated WUE from the ratio of cumulative GEP and cumulative ET during May–August for both the cottonwood and grassland sites. In addition, daily average ecosystem WUE ( $\text{mmol mol}^{-1}$ ) was calculated as the ratio of GEP to ecosystem ET in June–July (days 152–212), when the ecosystem was near peak photosynthetic activity. These daily average calculations made use of the half-hour time periods between 10:00 and 17:00 h at both sites when air temperature and VPD were high, and near the daily maximum (see Table 1 for average air temperature and VPD values that were apparent during the time periods used for these calculations). To reduce the contribution of the evaporation component of ET, days with recorded precipitation were excluded. In addition, we also excluded any time periods with low ET fluxes ( $0.05 \text{ mmol m}^{-2} \text{ s}^{-1}$ ) and inadequate turbulence ( $u^* < 0.15 \text{ m s}^{-1}$ ), as described in Ponton et al. (2006). The number of days during June–July with available daily WUE values (sample size) differed among sites and years (forest sample size: 38, 59, 58; grassland sample size: 60, 60, 61; for 2014, 2015 and 2017, respectively). A two-way ANOVA for an unbalanced design (with type III sums of squares) was conducted to test the significance of “site” and “year” effects (and their interaction) on the daily WUE values averaged over June–July. A one-way ANOVA was used to test for significant differences among years for average air temperature and VPD conditions that were apparent during the time of daily WUE calculations (Table 1). These statistical tests were also conducted using Matlab software.

### 3. Results

#### 3.1. Comparison of environmental conditions

Total growing season (May–September) precipitation was higher in 2014 (363 mm) than normal ( $258 \pm 106 \text{ mm}$ , 30-year average  $\pm$  SD), near normal in 2015 (181 mm), and below normal in 2017 (125 mm) (Fig. 1). Extremely high rainfall of 144.5 mm during days 164–170 caused widespread over-bank flooding of the Oldman River in 2014 (Fig. 2). This flood was typical for floods of the area in that it was caused by heavy precipitation during late May to early July when soils of the upper watershed catchment were near saturation. Floods in the Oldman River watershed are generally not associated with inter-annual variation in snow-pack conditions (Rood et al., 1998, 2007).

The seasonal patterns for daily maximum and minimum air temperature were similar in 2014, 2015, and 2017, but the maximum temperatures increased progressively from 2014 through the two later years, particularly during July and August of 2017 when there was

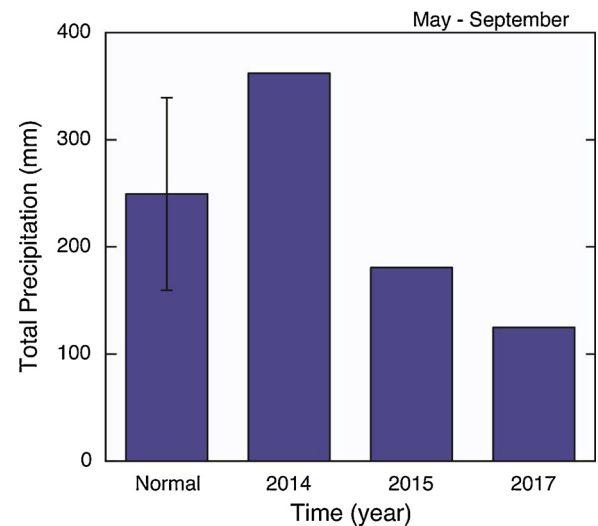


**Fig. 1.** Total precipitation recorded in Lethbridge, Alberta from May to September during 2014, 2015, 2017. The climate normal precipitation was the 30-year average  $\pm$  SD during 1971–2000 recorded at the Lethbridge airport.

almost no precipitation (Fig. 2, Table 1). Daily maximum VPD increased from May to September, and this growing season trend was stronger in 2017 than in the other two study years (Fig. 2, Table 1). Available soil moisture content was very high throughout the 2014 growing season at the cottonwood site because of the over-bank flooding of the adjacent Oldman River, but soil moisture declined progressively during the study period to values in 2017 that were only approximately 30% of maximum observed in 2014 (Fig. 2). Available soil moisture at the grassland site varied quite strongly within the growing season in all three study years in association with alternating times of precipitation inputs and periods with no rain (Fig. 2). However, time periods with relatively high soil water content at the grassland site were more frequent in 2014 and declined consistently from 2015 to 2017. Virtually all available soil moisture was exhausted at the grassland site by early July in 2017, and precipitation input during later July and August was too low to cause any substantial change in soil moisture content for the rest of the 2017 growing season (Fig. 2). The relatively high precipitation that occurred in early September 2015 at the grassland site resulted in a large increase in soil moisture content and a second pulse of new plant growth after the initial plant community had largely gone into a drought-induced dormancy (see further discussion on this below, associated with descriptions of data in Figs. 6 and 7).

#### 3.2. Ecosystem energy and water fluxes

The peak value of the July mean diurnal pattern for latent heat flux showed a progressive decline from 2014 through 2017 at both the cottonwood and grassland sites, although there was a larger decline apparent at the grassland site (Figs. 3 and 4). There were associated increases in the peak values of the diurnal pattern for sensible heat flux as latent heat flux declined at both study sites. At the cottonwood site, peak sensible heat flux was higher than peak latent heat flux only in July 2017, while at the grassland the peak sensible heat flux was higher than peak latent heat flux in July of both 2015 and 2017 (Figs. 3 and 4). Canopy conductance values in July, calculated from inversion of the Penman-Monteith equation, showed progressive declines from 2014 through 2017 at both study sites. The July maximum canopy conductance values were substantially higher at the cottonwood site than at the grassland site in all study years (Figs. 3 and 4).

The peak values and seasonal patterns for daily-integrated ET were similar in all study years at the cottonwood site, with only a relatively small reduction in daily ET values during July and August of 2017



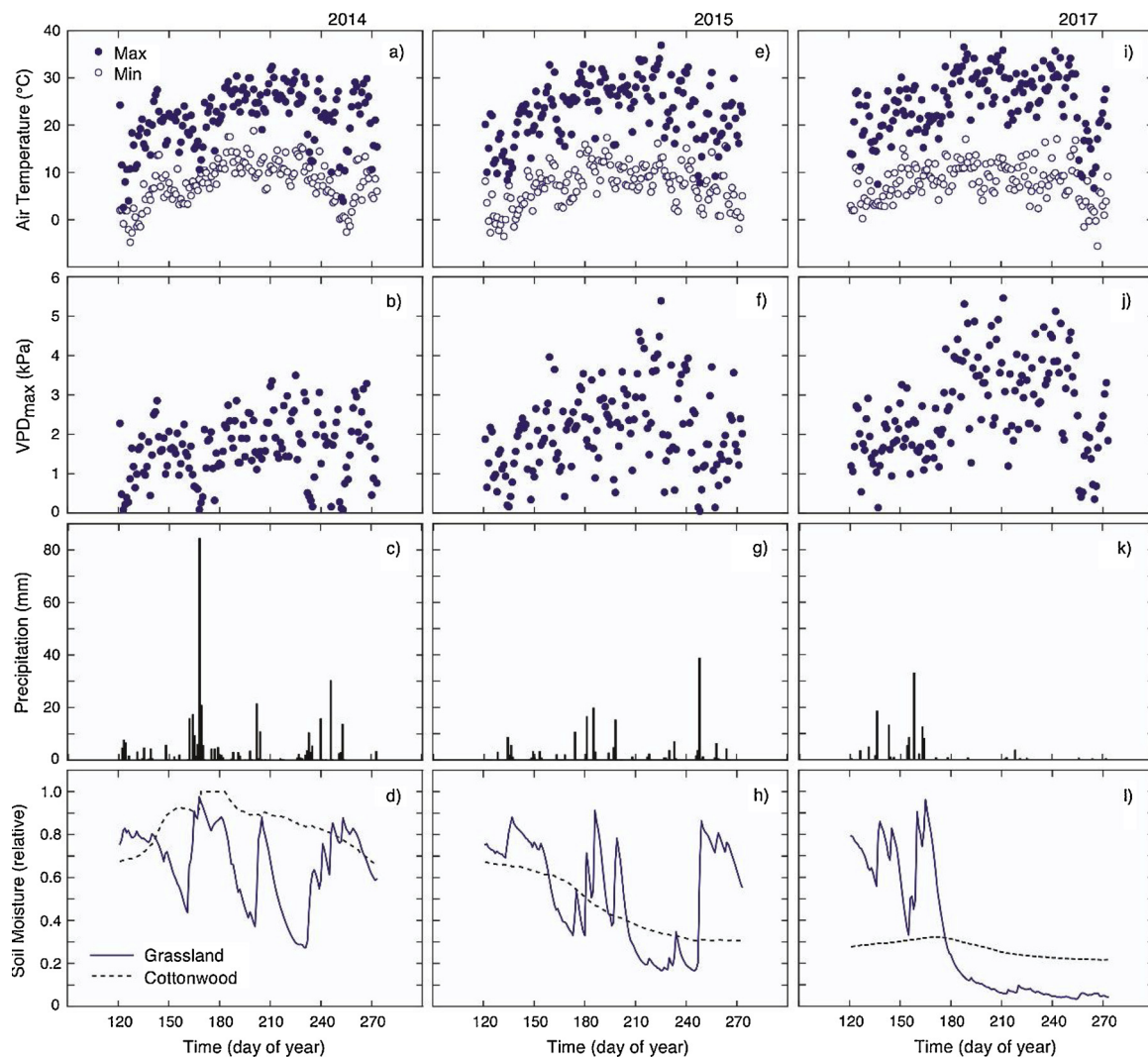


**Fig. 2.** Seasonal variation in the daily maximum and minimum air temperature (a, e, i), daily maximum vapor pressure deficit ( $VPD_{max}$ ) (b, f, j), daily total precipitation (c, g, k), and soil moisture content (d, h, l) at a cottonwood forest and a nearby grassland in Lethbridge, Alberta during 2014, 2015, 2017. Soil moisture content was expressed on a relative scale (0–1), as available soil moisture, calculated using the maximum and minimum volumetric water contents recorded at the two sites. Soil moisture measurements were integrated over 0–250 cm depth at cottonwood forest and over 0–15 cm depth at the grassland.

compared to values measured in 2014 (Fig. 5). The cumulative ET from May–September at the cottonwood site was also quite similar among study years (451 mm [2014], 411 mm [2015], 375 mm [2017]) (Fig. 5). While cumulative ET exceeded cumulative precipitation in all years at the cottonwood site, the difference between ET and precipitation was much larger in 2015 (230 mm) and 2017 (251 mm) than in 2014 (89 mm) (Fig. 5).

The peak values and seasonal patterns for daily-integrated ET differed among study years at the grassland site (Fig. 6). Maximum ET values at the grassland declined from 2014 through to 2017, in association with the lower precipitation inputs and reduced soil moisture during 2015 and 2017 (Fig. 2). In addition, the active time period with high ET rates was progressively lower in 2015 and 2017 relative to 2014 (Fig. 6). A second peak of ET activity occurred in early September 2015 (Fig. 6), in association with a second pulse of new plant growth stimulated by significant precipitation input at this time (Fig. 2). Cumulative ET during May–September at the grassland varied strongly among study years (213 mm [2014], 160 mm [2015], 111 mm [2017]), and was lower than cumulative precipitation input in all years (Fig. 6). The seasonal pattern of grassland cumulative ET closely followed the pattern of cumulative precipitation input in 2015 and 2017 (Fig. 6). In 2014 the seasonal pattern of cumulative ET also followed cumulative

precipitation inputs, with the exception that the extremely high rainfall during days 164–170 did not stimulate similar increases in ET, and this short pulse of precipitation was likely lost as runoff (Fig. 6).

### 3.3. Ecosystem photosynthesis and water use efficiency

Ecosystem photosynthesis (GEP) showed similar patterns of seasonal variation as that illustrated for ET for both the cottonwood and grassland ecosystems (Figs. 5–7). In addition, the peak GEP values and the seasonal patterns of GEP variation were very similar among years at the cottonwood site (Fig. 7). At the grassland site, maximum GEP was only approximately 50% of that recorded at the cottonwood forest (Fig. 7a,b). The seasonal peak values of GEP at the grassland site declined from 2014 to 2017, and the active time period with high GEP values was much shorter in 2015 and 2017 than in 2014 (Fig. 7). In addition, the peak GEP values at the grassland occurred earlier in 2015 and 2017 compared to 2014. The contrasting peak values and seasonal patterns of GEP contributed to the large differences observed between sites in the growing season cumulative GEP (Fig. 8a). The May–August cumulative GEP was very similar among years at the cottonwood site ( $1176 \text{ g C m}^{-2}$  [2014],  $1137 \text{ g C m}^{-2}$  [2015],  $1222 \text{ g C m}^{-2}$  [2017]), while cumulative GEP values at the grassland in 2015 ( $321 \text{ g C m}^{-2}$ )

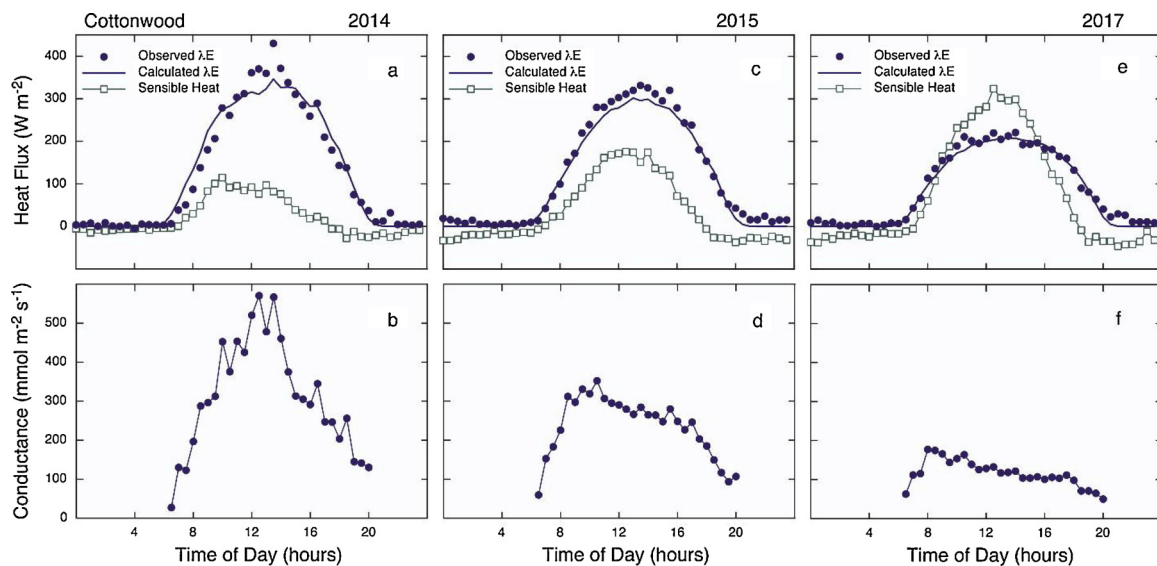


**Fig. 3.** Mean diurnal patterns in July for measured latent heat flux ( $\lambda E$ ) and sensible heat flux (a, c, e), and calculated canopy conductance (b, d, f), at a cottonwood forest in Lethbridge, Alberta during 2014, 2015, 2017. The solid blue lines in component figures a, c, and e were calculated using the Penman-Monteith equation. Data from figures a–d were originally presented in Flanagan et al. (2017). (For interpretation of the references to colour in this figure legend, the reader is referred to the web version of this article).

and 2017 ( $325 \text{ g C m}^{-2}$ ) were only approximately 57% of that recorded in 2014 ( $564 \text{ g C m}^{-2}$ ; Fig. 8a).

We calculated growing season average ecosystem WUE using two approaches, the first was based on the ratio of cumulative GEP and ET during May–August (Fig. 8), and the second on the average daily WUE calculated during mid-day (10:00 to 17:00 h) in June and July (Fig. 9). Ecosystem WUE values calculated with the first approach were similar among all three years at the cottonwood site; the slightly higher WUE calculated for the cottonwood site in 2017 was primarily due to lower cumulative ET in that year (Fig. 8). Grassland WUE values were lower than those calculated for the cottonwood site in all years based on cumulative values of GEP and ET (Fig. 8c). In addition, grassland WUE was lower in 2015, and marginally higher in 2017 compared to the WUE calculated for the grassland in 2014 (Fig. 8c).

Site, year and their interaction were all statistically significant effects based on a two-way ANOVA for the average daily WUE values

shown in Fig. 9. The grassland had significantly lower WUE than the cottonwood forest in June–July of 2015 and 2017, but the small difference in average WUE between sites during 2014 was not statistically significant (Fig. 9).

#### 4. Discussion

This comparative study between native grassland and riparian forest ecosystems, which were exposed to the same aboveground environmental conditions, allowed for evaluation of other dominant factors including plant functional type, LAI and soil and groundwater access for their effects on ecosystem water-use and WUE. In addition, the contrasting environmental conditions among study years provided insights into mechanisms that control water-use and WUE in the two ecosystems. Such comparative studies of water-use are important for helping to understand how ecosystem carbon and energy budgets will be

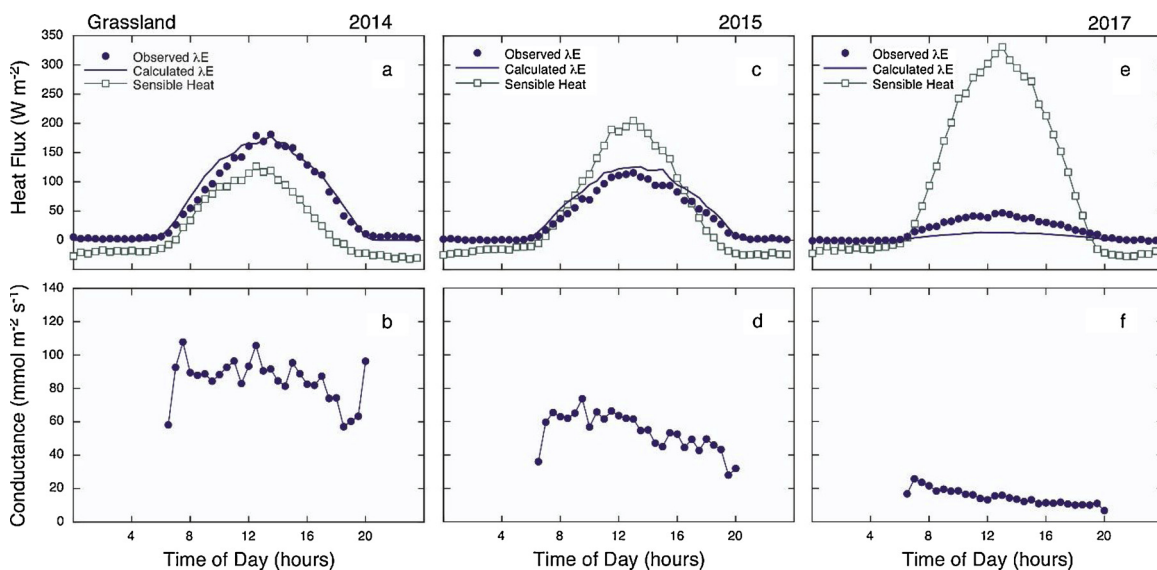


**Fig. 4.** Mean diurnal patterns in July for measured latent heat flux ( $\lambda E$ ) and sensible heat flux (a, c, e), and calculated canopy conductance (b, d, f), at a grassland in Lethbridge, Alberta during 2014, 2015, 2017. The solid blue lines in component figures a, c, and e were calculated using the Penman-Monteith equation (For interpretation of the references to colour in this figure legend, the reader is referred to the web version of this article).

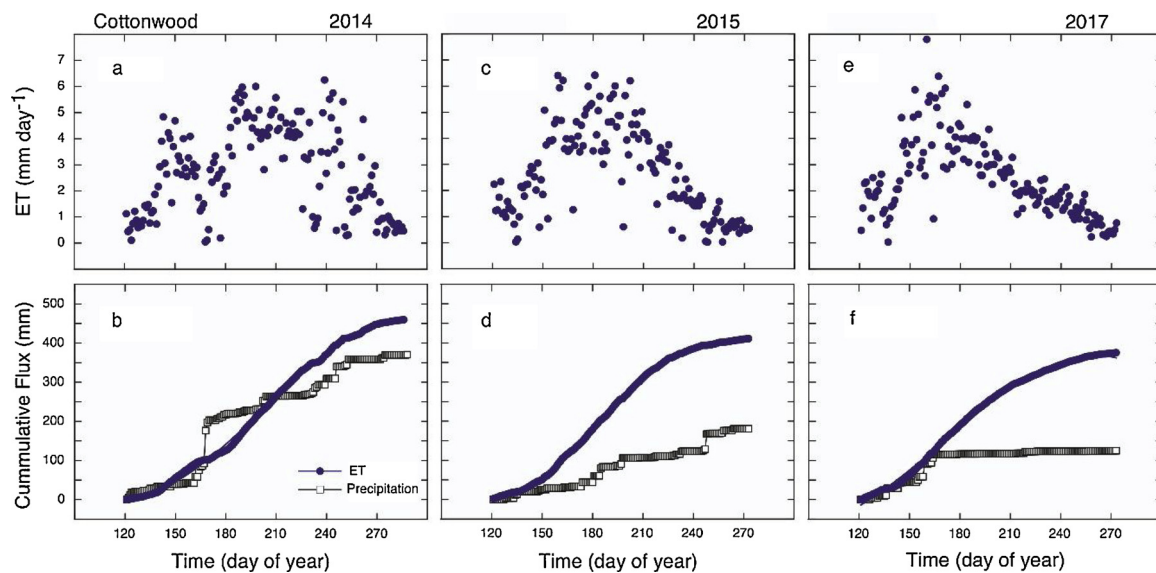


Fig. 5. Seasonal variation in the daily evapotranspiration (ET) rates (a, c, e) and cumulative ET (solid blue circles) and cumulative precipitation (open black squares) (b, d, f) at a cottonwood forest in Lethbridge, Alberta during 2014, 2015, 2017. Data from figures a–d were originally presented in Flanagan et al. (2017). (For interpretation of the references to colour in this figure legend, the reader is referred to the web version of this article).

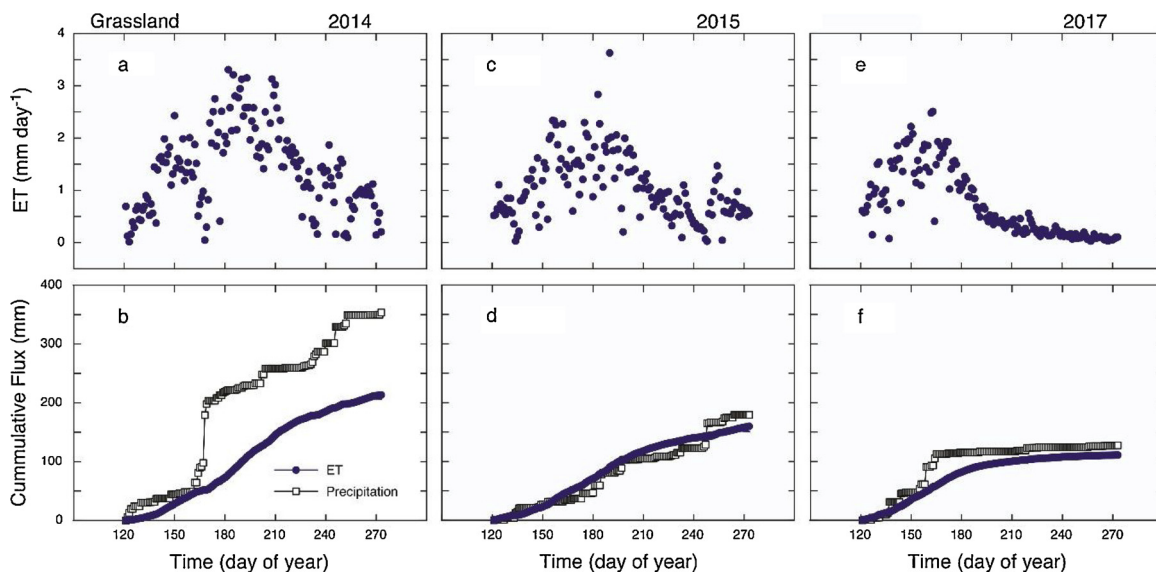


Fig. 6. Seasonal variation in the daily evapotranspiration (ET) rates (a, c, e) and cumulative ET (solid blue circles) and cumulative precipitation (open black squares) (b, d, f) at a grassland in Lethbridge, Alberta during 2014, 2015, 2017 (For interpretation of the references to colour in this figure legend, the reader is referred to the web version of this article).

influenced by climate change and by the management of regulated river flow patterns associated with dam operation.

#### 4.1. Ecosystem water-use

Growing season (May–September) cumulative ET was very similar to cumulative precipitation input at the grassland during 2015 and 2017 (Fig. 6d, f). In 2014, however, cumulative precipitation exceeded cumulative ET by 150 mm, an amount that was similar to the large rainfall event of 144.5 mm during days 164–170 that caused widespread over-bank flooding of the Oldman River (Fig. 2). After subtracting this pulse of precipitation, much of which was likely lost as runoff, the seasonal pattern of cumulative ET also closely followed cumulative precipitation inputs in 2014 at the grassland (Fig. 6b). Consistent with previous analyses conducted at this study site (Wever et al., 2002), grassland ecosystem water-use depended primarily on precipitation inputs during

the growing season to supply the necessary soil moisture. It is possible, however, for some carry-over of soil moisture from the previous year's growing season to influence water-use and productivity in a subsequent year, but this does not occur every year at this grassland study site (Flanagan and Adkinson, 2011). The shallow soil at the grassland results in relatively low water storage capacity (field capacity minus wilting point,  $420 - 160 = 260$  mm; Hufkens et al., 2016), an amount that was similar to the 30-year average precipitation input during May–September (Fig. 1).

Seasonal peak values of mid-day ET (approximately  $6 \text{ mm day}^{-1}$ ; Fig. 5) in the cottonwood forest were on the low end of the range of peak daily values ( $6\text{--}10 \text{ mm day}^{-1}$ ) for ET in riparian *Populus* ecosystems in New Mexico and California (Cleverly et al., 2006; Nagler et al., 2007). The cumulative ET during the growing season at the cottonwood site was quite similar among study years and it exceeded seasonal cumulative precipitation inputs in all years (Fig. 5). The water required



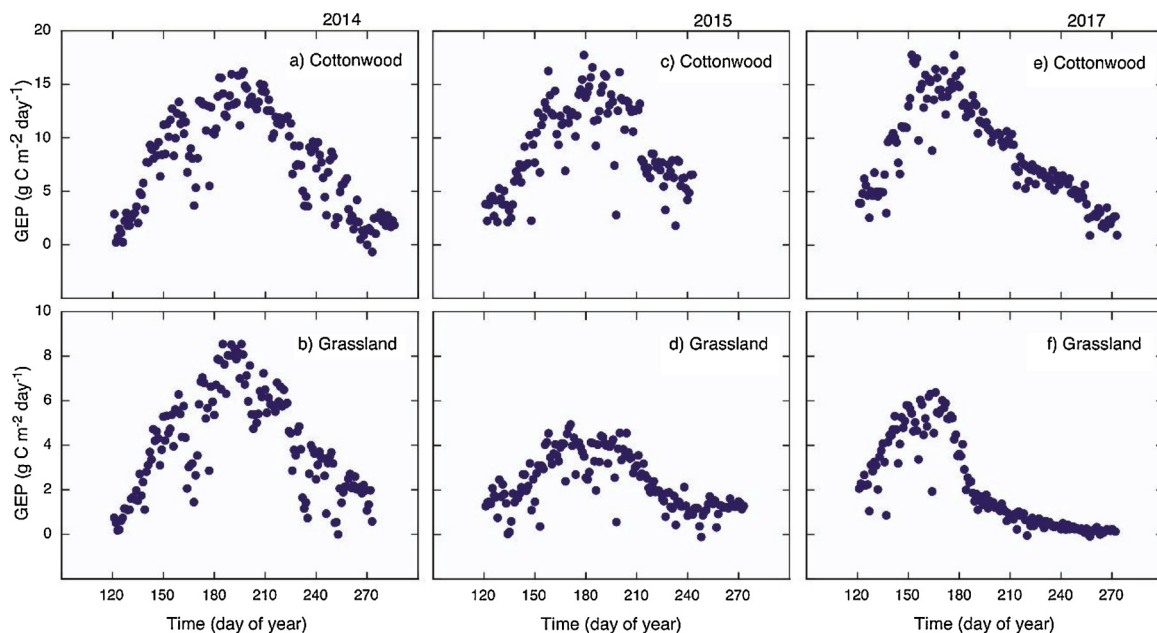


Fig. 7. Seasonal variation in the daily-integrated gross ecosystem photosynthesis (GEP) rates at a cottonwood forest (a, c, e) and a nearby grassland (b, d, f) in Lethbridge, Alberta during 2014, 2015, 2017. Data from figures a and c were originally presented in Flanagan et al. (2017).

for ET, that exceeded growing season precipitation, could be provided by soil water storage or by access to alluvial groundwater. Soil at the cottonwood forest (2.5 m depth) had a relatively large water storage capacity (approximately 1300 mm, Flanagan et al., 2017), and 22–32% (286–416 mm) of this soil water capacity was available even during the dry 2017 growing season (Fig. 2). The difference between the maximum ( $A_w = 0.32$ ) and minimum ( $A_w = 0.22$ ) soil water contents recorded in 2017 was equivalent to approximately 130 mm of water (Fig. 2). If all that seasonal change in soil water content (130 mm) was used in ET, along with all of the precipitation input during May–September (125 mm), an additional supply of 120 mm would have been required from alluvial groundwater sources to support the observed cumulative ET of 375 mm in 2017 at the cottonwood site. This should be a very conservative estimate of the alluvial groundwater used in ET, because seasonal changes in soil water content at this site are also strongly influenced by seasonal changes in the flow rate of the adjacent Oldman River, which is a “losing river” that contributes to the riparian forest soil water storage capacity as the river level fluctuates (Rood et al., 2013; Flanagan et al., 2017). So both the large soil water storage capacity and access to alluvial groundwater by deep-rooted, phreatophytic trees supported the relatively consistent and high cumulative ET recorded at the cottonwood site during the three study years (Fig. 5).

#### 4.2. Ecosystem water-use efficiency

We used two approaches to calculate ecosystem WUE, and both calculation procedures produced similar values of WUE (Figs. 8 and 9). However, the first approach (Fig. 8c) resulted from an integrated perspective on GEP and ET during the majority (May–August) of the potential growing season, which can extend from May to September in years with favorable environmental conditions. In contrast, the second approach (Fig. 9) focused on processes only at mid-day during peak photosynthetic activity in June and July, and so it was not as strongly influenced by differences in the inter-annual variation in the seasonal timing of GEP and ET that were very pronounced at the grassland site (Figs. 5–7). Instead, the second approach for calculating WUE was more strongly influenced by leaf-level photosynthetic characteristics and maximum LAI than by variation in the seasonal timing of GEP and ET.

At the leaf level, WUE is controlled by the ratio of photosynthetic carbon uptake ( $A$ ) and stomatal conductance to water loss ( $g$ ), or

intrinsic water-use efficiency ( $A/g$ ). Plants with different life histories or contrasting plant functional types show systematic variation in  $A/g$  when grown under similar environmental conditions, and grasses tend to have lower  $A/g$  values than broad-leaf deciduous trees (Smedley et al., 1991; Brooks et al., 1997). These expected differences in leaf gas exchange characteristics likely contributed to the lower ecosystem WUE we observed for the grassland relative to the cottonwood forest site (Figs. 8c and 9). In addition, the lower maximum LAI at the grassland site allowed for greater solar radiation input to the soil surface and may have increased soil evaporation and ET relative to GEP, which would also contribute to the lower WUE observed at the grassland site. The WUE values we measured for the cottonwood site ( $4.4\text{--}5.3 \text{ mmol mol}^{-1}$ , based on cumulative GEP and ET) were very similar to WUE values ( $4.5\text{--}5.4 \text{ mmol mol}^{-1}$ ) measured for an aspen forest (*Populus tremuloides*) in Saskatchewan (Arain et al., 2002; Ponton et al., 2006). In addition, the WUE values we measured based on cumulative GEP and ET at the grassland site ( $3.0\text{--}4.4 \text{ mmol mol}^{-1}$ ) were similar but slightly higher than WUE values ( $2.6\text{--}3.1 \text{ mmol mol}^{-1}$ ) measured at the same site in different years (Wever et al., 2002; Ponton et al., 2006; Flanagan and Farquhar, 2014).

At the cottonwood site there were only minor differences apparent among years for WUE (Figs. 8c and 9). The small increase in WUE during 2017 was a result of slightly lower ET in that year, while cumulative GEP remained approximately equal during all study years at the cottonwood site (Fig. 8). Canopy conductance was markedly reduced in 2017 compared to 2014 and 2015 at the cottonwood site (Fig. 3), and this was likely the major reason for the slightly lower cumulative ET and higher WUE during 2017. We speculate that most of the reduction in canopy conductance was a result of reduced photosynthetic gas exchange in shallowly rooted understory plants at the cottonwood site associated with low precipitation in 2017, and was not due to substantially lower photosynthetic activity in the cottonwood trees. Total LAI (1.8) is split equally between cottonwood trees (0.9) and understory plants (0.9) at this site (Flanagan et al., 2017). Lower rates of soil evaporation, due to reduced surface water input from precipitation at the cottonwood site, may have also contributed to the lower ET and higher WUE during 2017.

There was relatively large inter-annual variation in WUE at the grassland site, with significantly lower WUE recorded in June–July of 2015 and 2017 compared to 2014 (Fig. 9). Interacting effects of



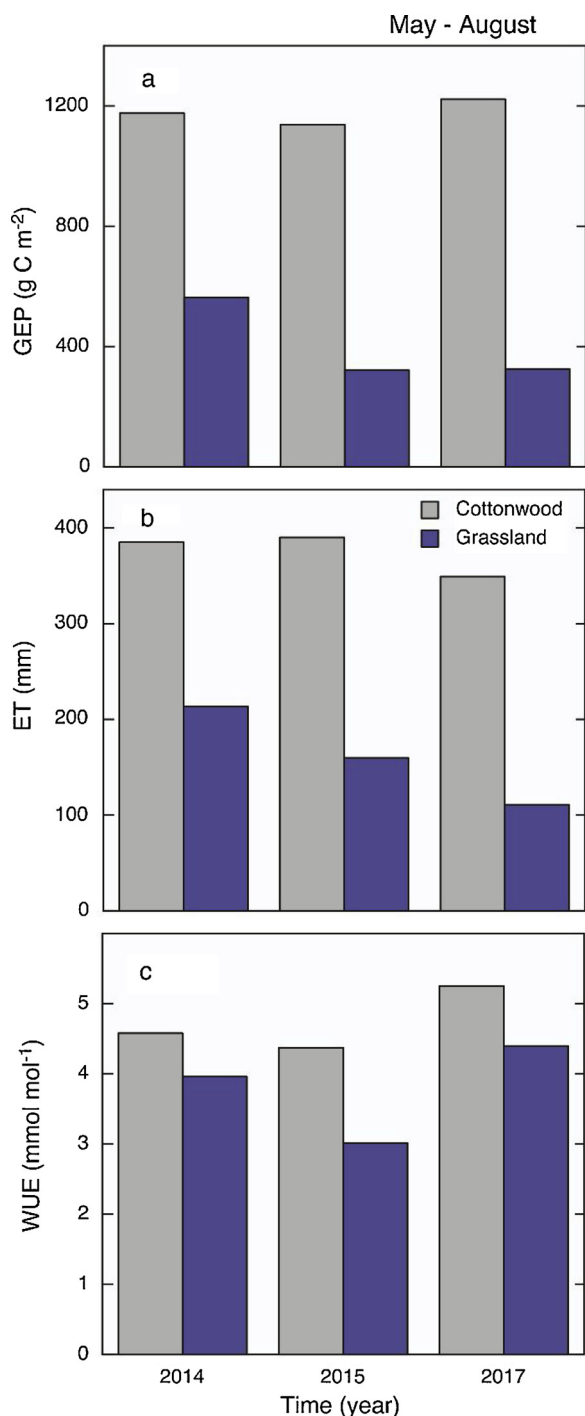


**Fig. 8.** Cumulative values during May-August for (a) ecosystem photosynthesis (GEP, g C m<sup>-2</sup>), (b) cumulative ecosystem evapotranspiration (ET, mm) and (c) seasonal ecosystem water-use efficiency (WUE, mmol mol<sup>-1</sup>, ratio of cumulative GEP and ET) in a cottonwood forest and grassland in Lethbridge, Alberta during 2014, 2015, 2017.

environmental variation among years and peak GEP values combined to result in higher WUE in 2014 compared to 2015 and 2017. Peak GEP values were reduced in both 2015 and 2017 compared to 2014 because of reduced precipitation, but peak GEP was higher in 2017 than 2015 despite the drier conditions in 2017 (Fig. 7). The warmer conditions, combined with sufficient precipitation and soil moisture during the start of the growing season (May-June), resulted in earlier leaf development and higher peak GEP in 2017 compared to 2015 (Figs. 2,7). However, leaf senescence occurred earlier in 2017 than 2015, so the

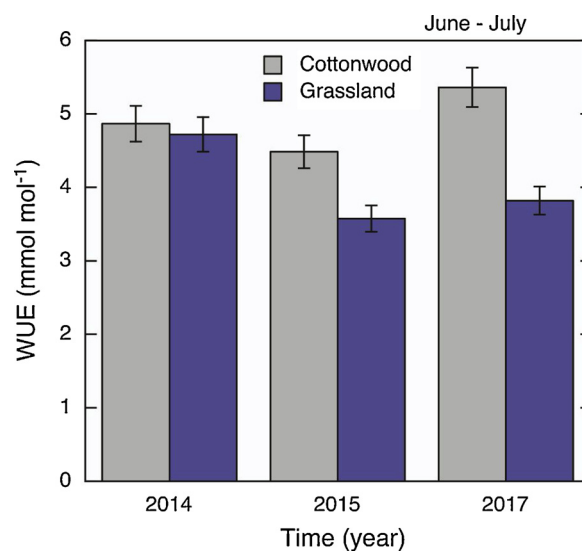


**Fig. 9.** Average ( $\pm$  SE) daily water-use efficiency for the cottonwood forest and grassland ecosystems at mid-day (10:00 to 17:00 h) in June-July (days 152–212) in Lethbridge, Alberta during 2014, 2015, 2017. Statistical significance was based on two-way ANOVA [Site effect,  $F(1, 330) = 52.6$ ,  $P < 0.001$ ; Year effect,  $F(2, 330) = 14.8$ ,  $P < 0.001$ ; Interaction,  $F(2, 330) = 10.9$ ,  $P < 0.001$ ].

total length of the growing season at the grassland was shorter in 2017 than in 2015 (Fig. 7). The higher peak GEP could have contributed to higher WUE in 2017 relative to 2015, but this was opposed by higher VPD conditions in 2017 (Table 1; Ponton et al., 2006) which stimulated ET and resulted in almost equal WUE occurring during June-July of 2015 and 2017 (Fig. 9). The higher peak GEP (Fig. 7) and lower VPD conditions (Table 1, Fig. 2) apparent in 2014 resulted in higher average mid-day WUE in June-July of that year compared to 2015 and 2017 (Fig. 9).

The pattern of variation in WUE observed among years at the grassland was different for the two procedures used to calculate WUE (Figs. 8c, and 9). As discussed above, this resulted from contrasting, seasonal variation in GEP and ET apparent among the different study years at the grassland site. Cumulative GEP values were almost identical in 2015 and 2017 despite the differences observed in peak GEP during these two years (Figs. 7 and 8). The longer time period of photosynthetic activity compensated for the lower peak GEP in 2015, relative to values observed in 2017. While cumulative GEP values were almost identical, cumulative ET was lower in 2017 than in 2015, and so WUE integrated over May-August was higher in 2017 than 2015 (Fig. 8). The flexible timing of plant growth in grasslands, and the warm conditions with sufficient soil moisture early in the 2017 growing season resulted in the higher, seasonal-integrated WUE in 2017 compared to 2015 (Fig. 8). The importance of interacting effects of temperature and soil moisture on the timing of leaf development, maximum LAI produced, and associated changes in ET and GEP have been noted previously at this site (Flanagan and Adkinson, 2011) and for grasslands in general (Hufkens et al., 2016).

#### 4.3. Conclusions

Our measurements indicated that cumulative growing season ET at the cottonwood site exceeded grassland ET by 2.1- to 3.4-fold depending on study year, despite slightly higher WUE in the cottonwood ecosystem. The absolute difference in cumulative ET between ecosystems ranged from 238 to 264 mm in different years, in a region that normally receives 258 mm of cumulative precipitation during May-September (Fig. 1). The relatively large ET at the cottonwood site was caused by higher LAI (approximately 2-fold higher), and associated

greater canopy conductance than was apparent at the grassland site. The additional soil water required to support the higher cottonwood ET was supplied by access to the semi-saturated capillary fringe above the alluvial groundwater table, and was also supported by a larger soil volume to store water from precipitation and river flooding inputs. These factors resulted in a relatively long time period for cottonwood canopy photosynthetic gas exchange that was very consistent among years despite widely different environmental conditions (Fig. 2, Table 1), while the grassland had shorter growing season lengths that were constrained further as precipitation and soil moisture declined among years. Our comparative analyses of water-use in these two ecosystems were consistent with the prediction that riparian cottonwood forests would be less sensitive to summer drought caused by low precipitation inputs than restricted access to alluvial groundwater associated with changes to adjacent river flow rates (Sperry and Love, 2015). Our analyses will help to improve management procedures for regulating the flow rates of southern Alberta rivers in order to sustain healthy riparian cottonwood ecosystems. This study also provides a research strategy that should be broadly applicable, and the findings provide guidance for water resource management in other semi-arid ecoregions where riparian cottonwood forests provide rich ecological resources that contrast within the otherwise treeless landscapes.

### Acknowledgements

This research was part of the *Functional Flows: A Practical Strategy for Healthy Rivers* project and was supported by grants from Alberta Innovates, the Natural Sciences and Engineering Council of Canada - Discovery Grant Program, and Conoco Phillips Canada. We thank Rachel Tkach, Lauren Schlerloski, Dylan Nikkel, Eric Sharp, Emily Wilton, Kayla Johnson, Caitlin Pelletier, Tyler Tremel, and David Pearce for help with some of the field and lab work. David Ellis (City of Lethbridge) and Coreen Putman (Helen Schuler Nature Centre, Lethbridge) provided permission to conduct research in the HSNR. Hao Yang was a visiting scholar at University of Lethbridge supported by the State Scholarship Fund from the China Scholarship Council (CSC).

### References

- Arain, M.A., Black, T.A., Barr, A.G., et al., 2002. Effects of seasonal and interannual climate variability on net ecosystem productivity of boreal deciduous and coniferous forests. *Can. J. For. Res.* 32, 878–891.
- Beer, C., Ciais, P., Reichstein, M., Baldocchi, D., Law, B.E., Papale, D., Soussana, J.-F., Ammann, C., Buchmann, N., Frank, D., Gianelle, D., Janssens, I.A., Knohl, A., Köstner, B., Moors, E., Rouspard, O., Verbeeck, H., Vesala, T., Williams, C.A., Wohlfahrt, G., 2009. Temporal and among-site variability of inherent water use efficiency at the ecosystem level. *Global Biogeochem. Cycles* 23 <https://doi.org/10.1029/2008GB003233>. GB2018.
- Brooks, J.R., Flanagan, L.B., Buchmann, N., Ehleringer, J.R., 1997. Carbon isotope composition of boreal plants: functional grouping of life forms. *Oecologia* 110, 310–311.
- Cleverly, J.R., Dahm, C.N., Thibault, J.R., McDonnell, D.E., Allred Coonrod, J.E., 2006. Riparian ecophysiology: regulation of water flux from the ground to the atmosphere in the Middle Rio Grande, New Mexico. *Hydrol. Process.* 20, 3207–3225.
- Flanagan, L.B., Adkinson, A.C., 2011. Interacting controls on productivity in a northern Great Plains grassland and implications for response to ENSO events. *Glob. Chang. Biol.* 17, 3293–3311.
- Flanagan, L.B., Farquhar, G.D., 2014. Variation in the carbon and oxygen isotope composition of plant biomass and its relationship to water-use efficiency at the leaf- and ecosystem-scales in a northern Great Plains grassland. *Plant Cell Environ.* 37, 425–438.
- Flanagan, L.B., Johnson, B.G., 2005. Interacting effects of temperature, soil moisture, and plant biomass production on ecosystem respiration in a northern temperate grassland. *Agric. For. Meteorol.* 130, 237–253.
- Flanagan, L.B., Wever, L.A., Carlson, P.J., 2002. Seasonal and interannual variation in carbon dioxide exchange and carbon balance in a northern temperate grassland. *Glob. Chang. Biol.* 8, 599–615.
- Flanagan, L.B., Orchard, T.E., Logie, G.S., Coburn, C.A., Rood, S.B., 2017. Water use in a riparian cottonwood ecosystem: eddy covariance measurements and scaling along a river corridor. *Agric. For. Meteorol.* 232, 332–348.
- Gom, L.A., Rood, S.B., 1999. Patterns of clonal occurrence in a mature cottonwood grove along the Oldman River, Alberta. *Can. J. Bot.* 77, 1095–1105.
- Harley, P.C., Thomas, R.B., Reynolds, J.F., Strain, B.R., 1992. Modelling photosynthesis of cotton grown in elevated CO<sub>2</sub>. *Plant Cell Environ.* 15, 271–282.
- Hauer, F.R., Locke, H., Dreitz, V.J., Hebblewhite, M., Lowe, W.H., Muhlfeld, C.C., Nelson, C.R., Proctor, M.F., Rood, S.B., 2016. Gravel-bed river floodplains are the ecological nexus of glaciated mountain landscapes. *Sci. Adv.* 2 e1600026.
- Heisler-White, J.L., Knapp, A.K., Kelly, E.F., 2008. Increasing precipitation event size increases aboveground net primary productivity in a semi-arid grassland. *Oecologia* 158, 129–140.
- Heisler-White, J.L., Blair, J.M., Kelly, E.F., Harmony, K., Knapp, A.K., 2009. Contingent productivity responses to more extreme rainfall regimes across a grassland biome. *Glob. Change Biol.* 15, 2894–2904.
- Hufkens, K., Keenan, T.F., Flanagan, L.B., Scott, R.L., Bernacchi, C.J., Joo, E., Brunsell, N.A., Verfaillie, J., Richardson, A.D., 2016. Productivity of North American grasslands is increased under future climate scenarios despite rising aridity. *Nat. Clim. Chang.* 6, 710–714.
- Jarvis, P.G., 1976. The interpretation of the variations in leaf water potential and stomatal conductance found in canopies in the field. *Philos. Trans. R. Soc. Lond., B, Biol. Sci.* 273, 593–610.
- Jarvis, P.G., McNaughton, K.G., 1986. Stomatal control of transpiration: scaling up from leaf to region. *Adv. Ecol. Res.* 15, 1–49.
- Katul, G., Leuning, R., Oren, R., 2003. Relationship between plant hydraulic and biochemical properties derived from a steady-state coupled water and carbon transport model. *Plant Cell Environ.* 26, 339–350.
- Keenan, T.F., Darby, B., Felts, E., Sonnentag, O., Friedl, M.A., Hufkens, K., O'Keefe, J., Klosterman, S., Munger, J.W., Toomey, M., Richardson, A.D., 2014. Tracking forest phenology and seasonal physiology using digital repeat photography. *Ecol. Appl.* 24, 1478–1489.
- Kellihfer, F.M., Leuning, R., Raupach, M.R., Schulze, E.-D., 1995. Maximum conductances for evaporation from global vegetation types. *Agric. For. Meteorol.* 73, 1–16.
- Knapp, A.K., Smith, M.D., 2001. Variation among biomes in temporal dynamics of aboveground primary production. *Science* 291, 481–484.
- Knapp, A.K., Beier, C., Briske, D.D., Classen, A.T., Luo, Y., Reichstein, M., Smith, M.D., Smith, S.D., Bell, J.E., Fay, P.A., Heisler, J.L., Leavitt, S.W., Sherry, R., Smith, B., Weng, E., 2008. Consequences of more extreme precipitation regimes for terrestrial ecosystems. *BioScience* 58, 811–821.
- Lloyd, J., 1991. Modelling stomatal responses in *Macadamia integrifolia*. *Aust. J. Plant Physiol.* 18, 649–660.
- Monteith, J.L., 1965. Evaporation and environment. The state and movement of water in living organisms. Symposium of the Society of Experimental Biology Vol. 19. Cambridge University Press, Cambridge, U.K, pp. 205–234.
- Nagler, P., Jetton, A., Fleming, J., Didan, K., Glenn, E., Erker, J., Morino, K., Milliken, J., Gloss, S., 2007. Evapotranspiration in a cottonwood (*Populus fremontii*) restoration plantation estimated by sap flow and remote sensing methods. *Agric. For. Meteorol.* 144, 95–110.
- Naiman, R.J., Décamps, H., McClain, M.E., 2005. Riparia: Ecology, Conservation, and Management of Streamside Communities. Elsevier, Amsterdam, the Netherlands.
- Ostlie, W.R., Schneider, R.E., Aldrich, J.M., Faust, T.M., McKim, R.L.B., Chaplin, S.J., 1997. The status of biodiversity in the Great Plains. *The Nature Conservancy, Arlington, VA, USA*, pp. 326 + xii.
- Ponton, S., Flanagan, L.B., Alstad, K.P., Johnson, B.K., Morgenstern, K., Kljun, N., Black, T.A., Barr, A.G., 2006. Comparison of ecosystem water-use efficiency among Douglas-fir forest, aspen forest and grassland using eddy covariance and carbon isotope techniques. *Glob. Change Biol.* 12, 294–310.
- Rood, S.B., Mahoney, J.M., Reid, D.E., Zilm, L., 1995. Instream flows and the decline of riparian cottonwoods along the St. Mary River, Alberta. *Can. J. Bot.* 73, 1250–1260.
- Rood, S.B., Kalischuk, A.R., Mahoney, J.M., 1998. Initial cottonwood seedling recruitment following the flood of the century of the Oldman River, Alberta, Canada. *Wetlands* 18, 557–570.
- Rood, S.B., Braatne, J.H., Hughes, F.M.R., 2003. Ecophysiology of riparian cottonwoods: streamflow dependency, water relations and restoration. *Tree Physiol.* 23, 1113–1124.
- Rood, S.B., Samuelson, G.M., Braatne, J.H., Gourley, C.R., Hughes, F.M.R., Mahoney, J.M., 2005. Managing rivers to restore floodplain forests. *Front. Ecol. Environ.* 3, 193–201.
- Rood, S.B., Goater, L.A., Mahoney, J.M., Pearce, C.M., Smith, D.G., 2007. Floods, fire, and ice: disturbance ecology of riparian cottonwoods. *Can. J. Bot.* 85, 1019–1032.
- Rood, S.B., Pan, J., Gill, K.M., Franks, C.G., Samuelson, G.M., Shepherd, A., 2008. Declining summer flows of Rocky Mountain rivers: historic hydrology and probable impacts on floodplain forests. *J. Hydrol. (Amst)* 349, 397–410.
- Rood, S.B., Ball, D.J., Gill, K.M., Kaluthota, S., Letts, M.G., Pearce, D.W., 2013. Hydrologic linkages between a climate oscillation, river flows, growth, and wood  $\Delta^{13}\text{C}$  of male and female cottonwood trees. *Plant Cell Environ.* 36, 984–993.
- Schindler, D.W., Donahue, W.F., 2006. An impending water crisis in Canada's western prairie provinces. *Proc. Natl. Acad. Sci. U. S. A.* 103, 7210–7216.
- Scott, R.L., Shuttleworth, W.J., Goodrich, D.C., Maddock, T., 2000. The water use of two dominant vegetation communities in a semiarid riparian ecosystem. *Agric. For. Meteorol.* 105, 241–256.
- Scott, R.L., Watts, C., Payan, J.G., Edwards, E., Goodrich, D.C., Williams, D., Shuttleworth, W.J., 2003. The understory and overstory partitioning of energy and water fluxes in an open canopy, semiarid woodland. *Agric. For. Meteorol.* 114, 127–139.
- Scott, R.L., Edwards, E.A., Shuttleworth, W.J., Huxman, T.E., Watts, C., Goodrich, D.C., 2004. Interannual and seasonal variation in fluxes of water and carbon dioxide from a riparian woodland ecosystem. *Agric. For. Meteorol.* 122, 65–84.
- Smedley, M.P., Dawson, T.E., Comstock, J.P., Donovan, L.A., Sherrill, D.E., Cook, C.S., Ehleringer, J.R., 1991. Seasonal carbon isotope discrimination in a grassland community. *Oecologia* 85, 314–320.
- Snyder, K.A., Williams, D.G., 2000. Water sources used by riparian trees varies among

- stream types on the San Pedro River, Arizona. *Agric. For. Meteorol.* 105, 227–240.
- Sperry, J.S., Love, D.M., 2015. What plant hydraulics can tell us about responses to climate change droughts. *New Phytol.* 207, 14–27.
- Wever, L.A., Flanagan, L.B., Carlson, P.J., 2002. Seasonal and interannual variation in evapotranspiration, energy balance and surface conductance in a northern temperate grassland. *Agric. For. Meteorol.* 112, 31–49.
- Wilcox, K.R., von Fischer, J.C., Muscha, J.M., Petersen, M.K., Knapp, A.K., 2015. Contrasting above- and belowground sensitivity of three Great Plains grasslands to altered rainfall regimes. *Glob. Chang. Biol.* 21, 335–344.
- Wong, S.C., Cowan, I.R., Farquhar, G.D., 1979. Stomatal conductance correlates with photosynthetic capacity. *Nature* 282, 424–426.
- Zhang, L., Wylie, B.K., Ji, L., Gilmanov, T.G., Tieszen, L.L., Howard, D.M., 2011. Upscaling carbon fluxes over the Great Plains grasslands: sinks and sources. *J. Geophys. Res.* 116, G00J03. <https://doi.org/10.1029/2010JG001504>.